Wireless Power and Data Telemetry with Push-Pull-Based Quadrature Modulation Scheme

Linran Zhao[1*], *Student Member, IEEE,* Yiming Han[1*], *Student Member, IEEE*, Bo-Ren Wang[1*], *Member, IEEE,* and Yaoyao Jia[1], *Member, IEEE*

[1]*Department of Electrical and Computer Engineering, The University of Texas at Austin.*

[*]Equally-Credit Authors (ECAs)

***Abstract*— This paper presents a wireless power and data telemetry circuit fabricated in a 180 nm CMOS process. The uplink data telemetry employs a push-pull-based quadrature (Q) modulation scheme that separates data and power transmissions onto the in-phase (I) and Q paths of the inductive link. By pushing or pulling energy from the secondary LC tank when the I-path power carrier is at 180°, a distinct data carrier is generated in the Q-phase. This orthogonal separation of power and data carriers effectively minimizes the impact of data transmission on wireless power transfer. The push-pull modulation inherently achieves both phase-shift keying and amplitude-shift keying to encode data using three symbols, enhancing the data rate. The proposed scheme transmits one symbol every two carrier cycles, breaking the trade-off between data rate and power transfer efficiency in conventional load-shift keying (LSK)-based telemetry. The back telemetry achieves a data rate of 10.17 Mbps on a 13.56 MHz inductive link with a power consumption of 98 µW, resulting in an energy efficiency of 9.63 pJ/bit.**

Keywords— wireless data transmission, wireless power, inductive link, quadrature modulation, back data telemetry, phase shift keying, implantable device

I. Introduction

Implantable devices show promising potential in scientific research, therapeutic development, health monitoring, and brain–machine interfaces [1], [2]. To make these devices fully implantable and reduce their invasiveness, they often incorporate wireless power and data transmission technologies. Wireless power eliminates the need for batteries, while bi-directional wireless communication enables the device to receive user commands via downlink (forward data telemetry) and transmit digitized physiological data via uplink (back data telemetry)—without the need for physical wires. Considering the stringent constraints on power and area at the implant side, both the downlink receiver and uplink transmitter must be highly efficient. While the downlink typically carries low-rate control signals, the uplink must support high-speed data transmission to continuously stream large volumes of real-time physiological data. Thus, the uplink has attracted growing attention in research focused on developing efficient, robust, and high data rate (DR) transmission methods.

A single inductive link, thanks to its high efficiency and low cost, is the most commonly used approach in recent wireless implantable devices for enabling both wireless power and data transmission. In such a configuration, as shown in Fig. 1a, a power amplifier (PA) drives a primary LC tank (L_1 and C_1) to resonate at a specific frequency (e.g., 13.56 MHz), thereby generating a magnetic field. This magnetic field induces an AC current in the secondary LC tank (L_2 and C_2), which is then converted to a DC supply to power the rest of the circuits in the implant. To transmit physiological data, conventional back telemetry commonly

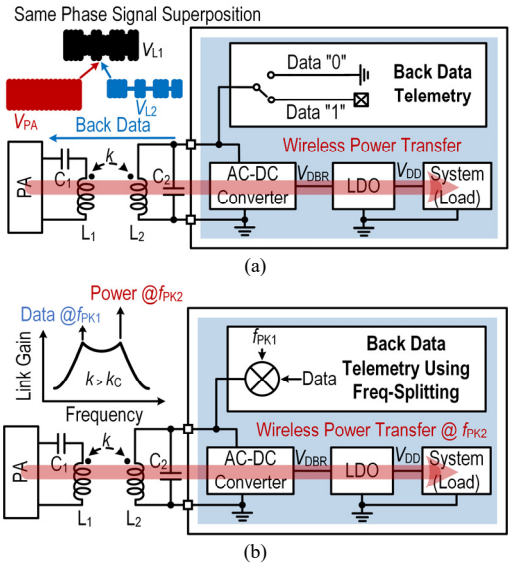

Fig. 1. Conventional back data telemetry over a single inductive link using (a) LSK modulation and (b) frequency-splitting method.

employs load shift keying (LSK) due to its simplicity and low power consumption [3-6]. Specifically, a switch is closed to short L_2 when transmitting a data "0," and opened to transmit a data "1." As a result, the voltage on the primary coil, V_{L1}, exhibits different amplitudes depending on the load associated with each bit. This allows the back data to be easily recovered by monitoring the amplitude of V_{L1}. Despite its simplicity, LSK has two key limitations. First, shorting the coil causes energy loss across the switch, significantly reducing power delivered to the load (PDL) and power transfer efficiency (PTE). Second, its maximum DR is inversely proportional to the link's quality factor, creating a trade-off between DR and PTE. To reduce energy loss, [6] proposed an energy-recycling modulation achieving 41% energy savings, but the DR-PTE trade-off limits its data transmission speed to less than 1 Mbps. In [3], cyclic on-off keying (COOK) breaks the DR-PTE trade-off and achieves 6.78 Mbps at a 13.56 MHz carrier but still results in substantial energy loss from periodic coil shorting.

Given the limitations in LSK, recent studies have explored leveraging the frequency-splitting characteristics of inductive link to separate the power and data carriers, as illustrated in Fig. 1b [7], [8]. This approach also extends the link bandwidth, enabling high DR and high PTE simultaneously. By combining frequency-splitting with quadrature phase shift keying (QPSK), [7] achieved 200 Mbps on a 390 MHz data carrier. However, this method requires the coupling coefficient (k) of two coils to exceed a critical threshold (k_C), imposing strict constraints on coils' alignment and distance. In addition, the positions of the two split frequency peaks are strongly dependent on the value of

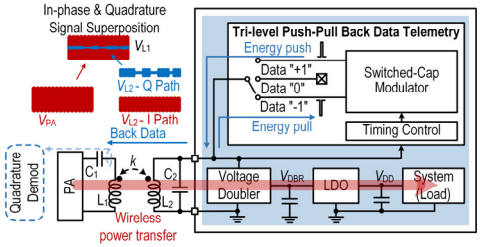

Fig. 2. Proposed back data telemetry using push-pull-based quadrature modulation scheme.

k, making data transmission highly sensitive to variations in k.

To address the limitations of conventional designs, this work proposes a push-pull-based quadrature modulation scheme. The push-pull operation separates power and data into two orthogonal paths: the in-phase (I-phase) for power and the quadrature-phase (Q-phase) for data path. When the I-phase power carrier reaches 180°, energy is either pushed into or pulled from the secondary LC tank. This operation generates a Q-phase signal for carrying back data, effectively separating power and data paths without requiring specific k of two coils. Additionally, the push-pull scheme forms a novel ternary constellation by leveraging both phase-shift keying (PSK) and amplitude-shift keying (ASK), thereby improving the DR. As a result, it avoids energy loss from coil shorting and breaks the traditional trade-off between DR and PTE. The proposed scheme achieves a state-of-the-art DR of 10.17 Mbps among all reported designs using 13.56 MHz carrier.

II. System Architecture and Circuit Implementation

Fig. 2 shows the block diagram of the proposed wireless power and data telemetry circuit and the overall wireless system. A PA drives the L_1 and C_1, resonating at 13.56 MHz, to deliver wireless power to L_2 and C_2. A voltage doubler converts the received AC power into a DC voltage, V_{DBR}, which is then regulated to a supply voltage, V_{DD}, by a low drop regulator (LDO) to power the remaining telemetry circuits. The back data telemetry, which consists of a switched-capacitor (SC) modulator and a timing control circuit, transmits the data by inducing and modulating the Q-phase data carrier. The data receiver picked up the modulated signal at PA side and decode the data using an in-phase and quadrature (I/Q) demodulator.

Fig. 3 illustrates the concept of the proposed quadrature modulation scheme. As shown in Fig. 3a, applying an energy impulse to an initially unexcited LC tank is able to generate an oscillating signal at its resonant frequency. Initially, the voltage across the LC tank, V_{LC}, is zero. After applying the positive impulse, V_{LC} rises to V_0 and begins to drop as the capacitor starts charging the inductor. Consequently, the induced resonating signal has an initial phase of 90°. As shown in Fig. 3b, when the impulse is applied at either 0° or 180° of the 13.56 MHz I-phase carrier (with 180° chosen in this design), the resulting oscillation retains the same frequency while shifting 90° relative to the I-phase carrier. This generates a Q-phase data carrier that is superimposed onto the inductive link with the I-phase power carrier. Because the back data is solely modulated on the orthogonal Q-phase signal, the amplitude of the I-phase power carrier remains minimized affected.

To enable data modulation on the Q-phase carrier, we implement a push-pull scheme that inherently realizes both

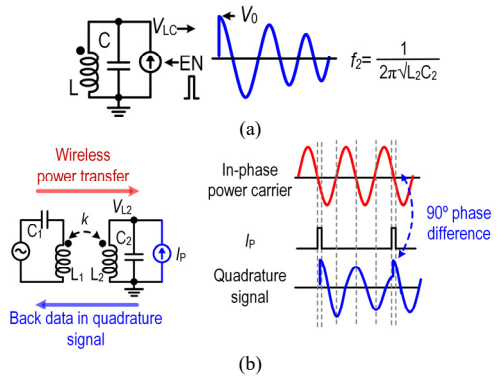

Fig. 3. (a) LC tank response to impulsive energy. (b) Generating a Q-phase signal from the power carrier via impulse.

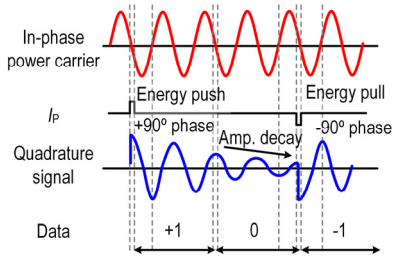

Fig. 4. Timing diagram of generating three symbols via push-pull scheme.

PSK and ASK. Unlike conventional binary modulation, this approach supports ternary signaling with three distinct symbols: "-1", "0", and "+1". Fig. 4 illustrates the detailed concept and timing of the push-pull modulation scheme. For data "1", an impulse pushed energy into the LC tank, resulting in a Q-phase signal with a -90° phase difference relative to the I-phase carrier. For data "-1", impulse pulled energy from the tank, producing the Q-phase signal with a +90° phase difference relative to the I-phase carrier. When the input is "0," impulse is not applied. In this way, data "0" can be distinguished from "±1" based on the amplitude of the Q-phase carrier, while "+1" and "-1" are differentiated by their phase. As a result, this scheme uses ASK to represent data "0," and PSK to encode data "±1". The push-pull operation occurs every two carrier cycles to reduce inter-symbol interference. With two cycles per symbol and ternary signaling, the proposed scheme improves the DR to 1.5 bits per two carrier cycle.

Fig. 5 shows the detailed circuit implementation of the proposed back telemetry which includes a SC modulator and timing control circuitry. In the timing control block, the zero-crossing detection circuit identifies every negative-going zero-crossing point of V_{L2} and generates a 6.78MHz clock signal. The clock signal is then provided to pulse generation circuit, which generates four control signals: Φ_{PS}, Φ_{PL}, Φ_{CH}, and Φ_{DIS}, depending on input data. These signals directly control four switches in the SC modulator to perform push, pull, or do-nothing operations. Fig. 6 illustrates the detailed timing of the SC modulator's operation. To transmit data "+1", the SC modulator pushes energy to the secondary LC tank. When V_{L2} crosses zero with negative slope, Φ_{PS} goes high while Φ_{CH} remains low, connecting a capacitor, C_{PS} and C_2 in parallel. Since C_{PS} is pre-charged and the voltage on C_2 is zero, a small amount of energy is pushed into the LC tank through capacitor charge sharing. After a short delay, Φ_{PS} goes low and Φ_{CH} goes high, allowing C_{PS} to be charged to V_{DBR} in preparation for the next energy push. To transmit data "-1", the SC modulator pulls energy from the secondary LC tank. A few ns before V_{L2} crosses zero from positive half-

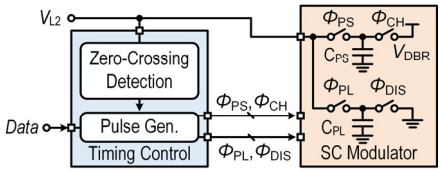

Fig. 5. Schematic of the timing control circuit and SC modulator.

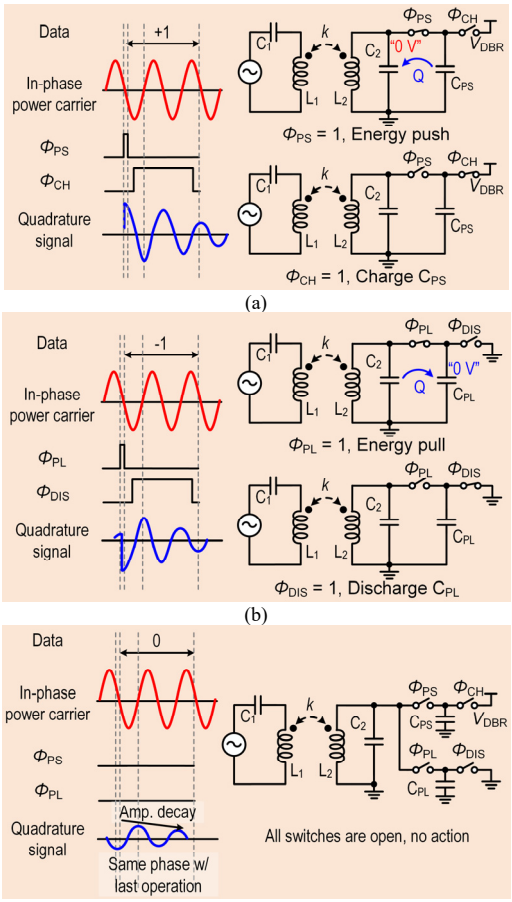

Fig. 6. Detailed operation of SC modulator when encoding data (a) "+1", (b) "-1", and (c) "0".

cycle, Φ_{PL} goes high while Φ_{DIS} remains low, connecting C_2 to an uncharged C_{PL}. This causes C_2 to share its charge with C_{PL}, effectively pulling energy from the LC tank. Once charge sharing is complete, Φ_{PL} goes low. Subsequently, Φ_{DIS} goes high to discharge C_{PL}, preparing it for the next energy pull. When input data is "0", all switches remain open, and no operation is performed on L_2 and C_2. As a result, the Q-phase signal continues to decay in amplitude while maintaining the same phase as the last energy push or pull operation.

III. Measurement Results

The wireless power and data telemetry circuit was fabricated using TSMC 180 nm CMOS process. The die micrograph in Fig. 7 shows its floor plan with a silicon area of 1.15 mm × 1.2 mm. Fig. 8 illustrates the bench-top testing setup. L_1 and L_2 were identically implemented using AWG-18 copper wire, achieving approximately 2 µH inductance and a quality factor of 180. C_1 and C_2 are 68 pF capacitors in 0603 package. To wirelessly power the circuit, a function generator (AFG31000) is used to excite the primary LC tank

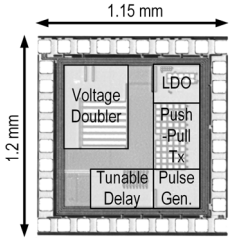

Fig. 7. Micrograph of the wireless power and data telemetry circuit.

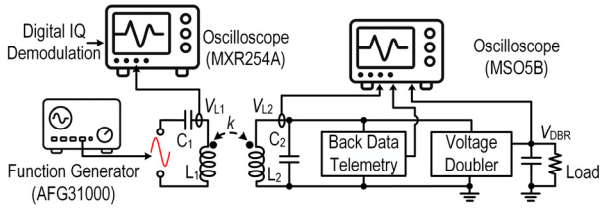

Fig. 8. Diagram of the bench-top testing setup.

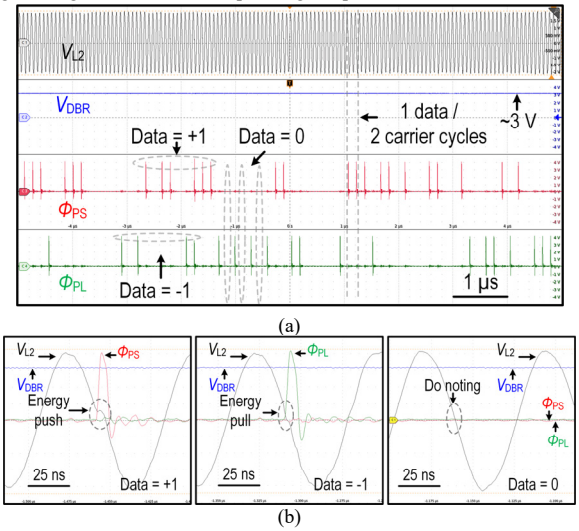

Fig. 9. Measured transient waveform showing the push-pull-based quadrature modulation scheme.

with a 13.56 MHz sinusoidal signal. To demonstrate the operation of the proposed push-pull scheme, an oscilloscope (MSO5B) is used to probe the V_{L2} along with the pulse signals, Φ_{PS} and Φ_{PL} generated by the telemetry circuit. A fixed 3 kΩ resistor is connected to the V_{DBR} to emulate load current. Meanwhile, V_{DBR} is probed to measure the real-time PDL through the inductive link. In addition, another oscilloscope (MXR254A) is utilized to probe V_{L1}, and digital I/Q demodulation is performed using Keysight 89600 Vector Signal Analyzer (VSA) software to verify successful data transmission.

Fig. 9a shows the transient waveform of the telemetry circuit, including V_{L2}, Φ_{PS}, Φ_{PL}, and V_{DBR}, to demonstrate the operation of the push-pull quadrature modulation scheme. L_2 receives wireless power and generates V_{L2} with an amplitude of approximately 4 V. Correspondingly, the voltage doubler produces a V_{DBR} of around 3 V. A pseudorandom ternary bit stream was fed to the telemetry circuit. The signals, Φ_{PS} and Φ_{PL} indicate energy push and pull operations for transmitting data "+1" and "-1", respectively. Fig. 9b zooms in on specific data transmission events. When Φ_{PS} goes high, the pre-charged C_{PS} pushes energy into C_2, resulting in a "pump" on V_{L2}. When Φ_{PL} is high, the empty C_{PL} pulls energy from C_2, causing a sudden drop on V_{L2}. Switching action does not occur when the input data is "0". To reduce inter-symbol

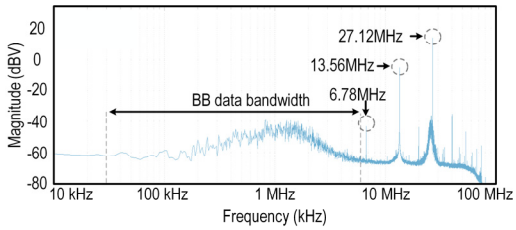

Fig. 10. Measured power spectrum of demodulated Q-phase signal.

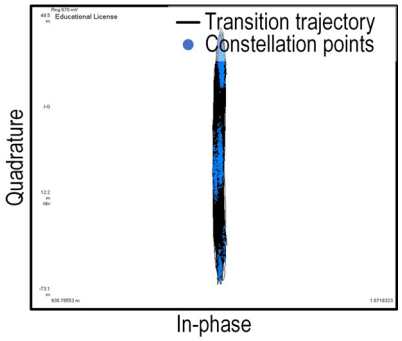

Fig. 11. Measured constellation diagram.

interference, the telemetry circuit transmits one data symbol every two carrier cycles. Considering the three-symbol modulation (encoded using two bits), the resulting DR is 10.17 Mbps.

To verify the successful push-pull-based data modulation of the proposed back telemetry, we performed Fast Fourier Transform (FFT) on the demodulated Q-phase signal. Fig. 10 shows the resulting power spectrum when a wideband pseudorandom bit stream is transmitted. The spectrum exhibits a strong and continuous energy distribution from approximately 30 kHz to 6 MHz, consistent with the expected bandwidth of the pseudorandom signal, thereby confirming successful data modulation. In addition, the wideband spectral content indicates that the transmitted data bandwidth is not limited by the quality factor of the inductive link. We also captured the constellation diagram, as shown in Fig. 11. Since the push-pull modulation scheme separates the I-phase for power transfer and the Q-phase for data transmission, the constellation points appear only along the Q-axis. The three distinct clusters correspond to the data symbols "+1", "0", and "-1", demonstrating the effectiveness of the proposed modulation scheme.

Table 1 compares the performance of the proposed wireless power and data telemetry circuit with state-of-the-art designs. The proposed push-pull quadrature modulation scheme enables the lowest symbol duration of just two carrier cycles. Consequently, it achieves the highest data rate of 10.17 Mbps among designs operating at a 13.56 MHz carrier frequency. This back telemetry consumes an average power consumption of 98 µW, resulting in an energy efficiency of 9.63 pJ/bit.

IV. Conclusion

This paper presents a wireless power and data telemetry circuit, equipped with a novel push-pull-based quadrature modulation scheme, enabling high-speed uplink over a 13.56 MHz inductive link for implantable device applications. The back telemetry uses a SC modulator to push or pull energy from the secondary LC tank when the I-phase power carrier reaches 180°, generating a separate data carrier in the Q-phase. In addition, the push-pull operation realizes simultaneous PSK and ASK, enabling ternary symbol encoding that improves both spectral efficiency and DR. The data telemetry transmits one symbol every two carrier cycles, achieving a 10.17 Mbps DR over the 13.56 MHz inductive link without compromising its PTE. Our push-pull approach effectively breaks the conventional trade-off between DR and PTE, enabling high-speed uplink over an inductive link. With average 98 µW power consumption, the data telemetry circuit achieves an energy efficiency of 9.63 pJ/bit.

Table I: Performance Comparison with State-of-the-Art Wireless Power and Data Telemetry Circuits

Reference	**This Work**	ISSCC 2025 [7]	TBioCAS 2024 [6]	JSSC 2023 [5]	JSSC 2019 [4]	JSSC 2016 [3]
Process	**180 nm**	65 nm	180 nm	180 nm	180 nm	65 nm
Data Transmission Scheme	**Push-Pull Quadrature Modulation**	LSK w/ Frequency-Splitting	LSK	Current-Modulated LSK	Load-Induced Resonant-Shift Keying	COOK
Modulation Scheme	**Combined PSK and ASK, 3 Symbols**	QPSK, 4 Symbols	Binary LSK, 2 Symbols	Binary LSK, 2 Symbols	Binary FSK, 2 Symbols	COOK, 4 Symbols
Carrier Freq. (MHz)	**13.56**	390	5	13.56	30	13.56
Carrier Cycles per Symbol	**2**	3.9	74.62	13.56	6	4
Symbol Rate / Data Rate (Mbps)	**6.78 / 10.17**	100 / 200	0.067 / 0.067	< 1 / < 1	5 / 5	3.39 / 6.78
Bit Error Rate	**< 10^{-10}**	<10^{-5}	<10^{-6}	2.1×10^{-6}	4.2×10^{-7}	9.9×10^{-8}
Power Consumption (µW)	**98**	N/A	N/A	630	395	64.44
Energy per Bit (pJ/bit)	**9.63**	0.67	N/A	> 630	79	9.5
Requires Specific k	**No**	Yes	No	No	No	No
WPT Power Loss due to Data Tx	**No**	No	Yes	No	Yes	Yes

References

[1] Madhvapathy, S.R., Bury, M.I., Wang, L.W. et al. "Miniaturized implantable temperature sensors for the long-term monitoring of chronic intestinal inflammation," *Nat. Biomed. Eng* 8, 1040–1052 (2024). https://doi.org/10.1038/s41551-024-01183-w

[2] Zhang, Y., Rytkin, E., Zeng, L. et al. "Millimetre-scale bioresorbable optoelectronic systems for electrotherapy," *Nature* 640, 77–86 (2025). https://doi.org/10.1038/s41586-025-08726-4

[3] S. Ha, C. Kim, J. Park, S. Joshi and G. Cauwenberghs, "Energy Recycling Telemetry IC With Simultaneous 11.5 mW Power and 6.78 Mb/s Backward Data Delivery Over a Single 13.56 MHz Inductive Link," in *IEEE Journal of Solid-State Circuits*, vol. 51, no. 11, pp. 2664-2678, Nov. 2016, doi: 10.1109/JSSC.2016.2600864.

[4] J. Pan, A. A. Abidi, W. Jiang and D. Marković, "Simultaneous Transmission of Up To 94-mW Self-Regulated Wireless Power and Up To 5-Mb/s Reverse Data Over a Single Pair of Coils," in *IEEE Journal of Solid-State Circuits*, vol. 54, no. 4, pp. 1003-1016, April 2019, doi: 10.1109/JSSC.2018.2888884.

[5] M. Kim, H. -S. Lee, J. Ahn and H. -M. Lee, "A 13.56-MHz Wireless Power and Data Transfer System With Current-Modulated Energy-Reuse Back Telemetry and Energy-Adaptive Voltage Regulation," in *IEEE Journal of Solid-State Circuits*, vol. 58, no. 2, pp. 400-410, Feb. 2023, doi: 10.1109/JSSC.2022.3207549.

[6] J. Lee, Y. Kim, D. Kang, I. Song and B. Lee, "A Reconfigurable Bidirectional Wireless Power and Full-Duplex Data Transceiver IC for Wearable Biomedical Applications," in *IEEE Transactions on Biomedical Circuits and Systems*, doi: 10.1109/TBCAS.2024.3483950.

[7] Y. Huang et al., "A Neuroprosthetic SoC with Sensory Feedback Featuring Frequency-Splitting-Based Wireless Power Transfer with 200Mb/s 0.67pJ/b Backscatter Data Uplink and Unsupervised Multi-Class Spike Sorting," *2025 IEEE International Solid-State Circuits Conference (ISSCC)*, San Francisco, CA, USA, 2025, pp. 272-274, doi: 10.1109/ISSCC49661.2025.10904677

[8] Y. Park et al., "A Wireless Power and Data Transfer IC for Neural Prostheses Using a Single Inductive Link With Frequency-Splitting Characteristic," in *IEEE Transactions on Biomedical Circuits and Systems*, vol. 15, no. 6, pp. 1306-1319, Dec. 2021, doi: 10.1109/TBCAS.2021.3135843